Anal. Chem. **2006,** *78,* 387−392

Articles

Hydrodynamic Dispersion in Shallow Microchannels: the Effect of Cross-Sectional Shape

Armand Ajdari,*,† Nathalie Bontoux,‡ and Howard A. Stone§

Laboratoire de Physico-Chimie Théorique, UMR 7083 CNRS-ESPCI, 10 rue Vauquelin, F-75231 Paris France, LPN-CNRS, Route de Nozay, Marcoussis 91460 France, and Division of Engineering and Applied Sciences, Harvard University, Cambridge, Massachusetts 02138

We highlight the fact that hydrodynamic dispersion in shallow microchannels is in most cases controlled by the width of the cross section rather than by the much thinner height of the channel. We identify the relevant time scales that separate the various regimes involved. Using the lubrication approximation, we provide simple formulas that permit a quantitative evaluation of dispersion for most shallow cross-sectional shapes in the "long-time" Taylor regime, which is effectively diffusive. Because of its relevance for microfluidic systems, we also provide results for the short-time "ballistic regime" (for specific initial conditions). The special cases of parabolic and quasi-rectangular shapes are considered due to their frequent use in microsystems.

Hydrodynamic dispersion refers to the inevitable spreading along the flow direction of dissolved or suspended Brownian particles in a flowing fluid, the ultimate origin of the spreading being related to velocity variations in the direction transverse to the mean flow. The effect is particularly significant in laminar flows in channels for which there is generally a gradual change in velocity from zero at the boundary to a maximum value in the center. The dispersion significantly reduces the resolution of analytic studies performed using pressure-driven flow in microfluidic devices and analytical lab-on-a-chip systems (ref 1 and references therein). Such analytic studies include, for example, separating species or determining rates of chemical reactions. Hydrodynamic dispersion also limits the number of samples that can be transported sequentially in a given microchannel and thereby limits the throughput of the device.

Although such (Taylor) dispersion is considered a well-understood phenomenon, it nevertheless remains difficult to quantify in practice for many microchannel configurations, which depart notably from the circular capillary usually described in textbooks. As a consequence, many analyses refer to situations with only one transverse dimension (radius or height), a procedure that we will show can lead to order of magnitude errors in the estimation of dispersion. In principle, the basic procedure for properly quantifying mass transport in laminar pressure-driven flows is well established, and follows the seminal works of Taylor[2] and Aris;[3] see also Brenner and Edwards.[4] Either of the two approaches, though somewhat different in detail, allows one to quantify the dispersion for arbitrary channel cross sections. In one recent application, Dutta and Leighton[5] discussed how to limit dispersion in pressure-driven flows by tailoring the cross-sectional shape of the microchannel. For simple shapes of the channel cross section (e.g., two planes, a circle, and an ellipse), analytical results for dispersion are available, while more complicated shapes require numerical analysis (see also ref 6).

In this paper, we provide basic results for describing simply and quantitatively the effect of hydrodynamic dispersion for situations where the microfluidic channel has a slender, shallow cross section with a typical height h_0 much smaller than the width w (see Figure 1, top). These situations are numerous in microfluidic devices, partly as a consequence of the various microfabrication methods (see, for example, ref 7 and references therein). Some common cross sections include quasi-rectangular and trapezoidal shapes (e.g., via chemical etching of crystalline silica), quasi-parabolic shapes (e.g., PDMS channels used in multilayer devices), etc.

There are two main contributions in this paper. First, we demonstrate and emphasize that, when $h_0 \ll w$, in almost all cases (i.e., we exclude quasi-rectangular cross sections) hydrodynamic dispersion is controlled by the width w, the larger of the two transverse dimensions, and not by the height h_0 of the microchannel. This fact is in contrast with calculations of the hydro-

* To whom correspondence should be addressed. E-mail: armand@turner.pct.espci.fr.

† Laboratoire de Physico-Chimie Théorique.

‡ LPN-CNRS.

§ Harvard University.

(1) Stone, H. A.; Stroock, A. D.; Ajdari, A. *Ann. Rev. Fluid Mech.* **2004**, *36*, 381−411.

(2) Taylor, G. I. *Proc. R. Soc., London Ser. A* **1953**, *219*, 186.

(3) Aris, R. *Proc. R. Soc. A* **1956**, *235*, 67−77.

(4) Brenner, H.; Edwards, D. A. *Macrotransport Processes*; Butterworth-Heinemann: Boston, MA, 1993.

(5) Dutta, D,; Leighton, D. T. *Anal. Chem.* **2001**, *73*, 504−513.

(6) Smith, R. *J. Fluid Mech.* **1990**, *214*, 211−228.

(7) Tabeling P. *Introduction à la microfluidique*; Paris, 2003.

10.1021/ac0508651 CCC: $33.50
Published on Web 12/06/2005

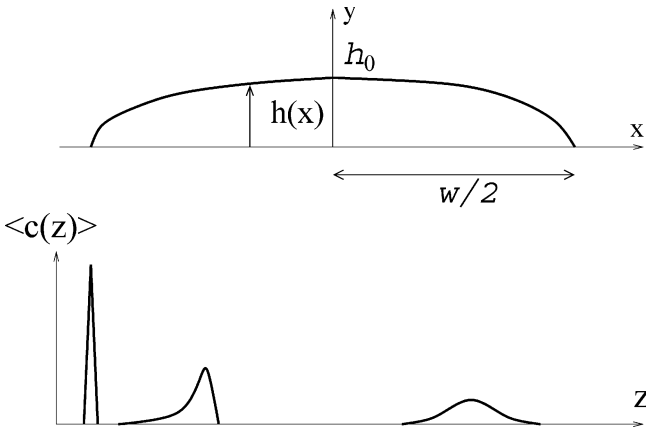

Figure 1. (Top) Cross section of a microchannel of arbitrary shape $y = h(x) = h_0H(x/(w/2))$. We focus on shallow channels for which $h_0 \ll w$, and estimate the spreading of a localized sample as it is convected downstream. (Bottom) Schematic of the spread of the cross-sectionally averaged concentration distribution as it moves downstream (z).

dynamic resistance, which is always controlled by the smallest of the two cross-sectional dimensions. Second, we provide simple (user-friendly) formulas for the hydrodynamic dispersion for any shape of the cross section, for the long-time Taylor dispersion regime, and also for the short-time regime of hydrodynamic stretching (focusing on specific initial conditions). Both time regimes are important in the microfluidic context, and our formulas also provide an estimate of the crossover time between the two regimes. These formulas are obtained following Aris's method of moments adapted to shallow geometries along the lines outlined at the end of his paper[3] and combining them with a lubrication description of the pressure-driven flow in these geometries.

For the sake of clarity, the paper is organized with the main results clearly identified and mathematical details relegated to the appendix. In the following section, we introduce the nomenclature used, comment on the physical ingredients of the problem, and provide the reader with our main results. We provide explicit formulas that exhibit the scaling dependence of the dispersion coefficient on the geometric and flow parameters and the quantitative dependence on the shape of the cross section. Following that, we discuss our results, compute the effective dispersion coefficients that quantify spreading for a variety of cross-sectional shapes, discuss the case of quasi-rectangular shapes, and comment on the implications of our results for microfluidic applications. In the Appendix, we provide the main lines of the derivation, which as mentioned above relies on Aris's "method of moments" formulation[3] combined with a lubrication description of pressure-driven flows in slender channels.

NOMENCLATURE AND MAIN RESULTS

Transport Model and Basic Definitions. Geometry. We utilize Cartesian coordinates and consider a straight channel of constant cross-sectional shape, with length L in the flow (z) direction, constant width w in the x direction, and a cross section described by its shape $h(x)$ in the y direction (Figure 1, top). The maximum value of $h(x)$ is denoted h_0. To conveniently discuss the scaling form of our results, we separate the amplitude h_0 from the specific "shape" of the cross section by writing $h(x) = h_0H(x/(w/2))$, where $H(X)$ is a dimensionless function that is zero for $X = \pm 1$ and has a maximum equal to 1 between these two points. We denote by S the constant cross-sectional area, $S = \int_{-w/2}^{w/2} h(x)\ \mathrm{d}x$. We present results valid for the conditions $h_0 \ll w \ll L$, which are generally true for a large number of microfluidic applications.

Flow and Transport of Particles. We assume that there is a steady incompressible pressure-driven laminar flow in the channel. The velocity field is directed along the channel axis, $\mathbf{u} = u(x, y)\mathbf{e}_z$, and this field is independent of z so long as the cross-sectional shape of the channel is constant. The cross-sectionally averaged (mean) velocity V is defined as

$$V = \frac{1}{S}\int_S u(x, y)\ \mathrm{d}S \tag{1}$$

We then consider a set of similar particles with a molecular (thermal) diffusivity D and describe their transport by the classical convective−diffusion equation for the concentration field $c(x, y, z, t)$:

$$\frac{\partial c}{\partial t} + \mathbf{u}\cdot\nabla c = D\nabla^2 c \tag{2}$$

We assume no flux boundary conditions at the walls of the channel, $\mathbf{n}\cdot\nabla c = 0$, where $\mathbf{n}$ is the local normal vector at the boundary.

Basic problem statement. We consider a sample of particles injected in the channel at time $t = 0$ and around $z = 0$ (initial concentration $c(x, y, z, t = 0)$), and we follow the evolution of this pulse (see Figure 1, bottom). The moments of the concentration distribution quantify the evolution:

$$\langle z^n\rangle(t) = \frac{\int z^n\left\{\int_{-w/2}^{w/2}\int_0^{h(x)} c(x, y, z, t)\ \mathrm{d}y\ \mathrm{d}x\right\}\mathrm{d}z}{\int\int_{-w/2}^{w/2}\int_0^{h(x)} c(x, y, z, t)\ \mathrm{d}y\ \mathrm{d}x\ \mathrm{d}z} \tag{3}$$

The innermost integrations in (3) provide the area-averaged concentration, which is often the quantity measured in experiments using a variety of detection schemes (refractometry, fluorescence, etc.). The mean position and variance are then $\langle z\rangle(t)$ and $\sigma^2(t) = \langle z^2\rangle(t) - \langle z\rangle^2(t)$. It is also common to quantify dispersion along the flow direction in terms of the (time dependent) effective dispersion coefficient, $D_{\mathrm{eff}}(t)$, defined as

$$D_{\mathrm{eff}}(t) = \frac{1}{2}\frac{\mathrm{d}}{\mathrm{d}t}\sigma^2(t) \tag{4}$$

which tends to a constant value at long times.[2]

Time Scales and Different Regimes for Shallow Channels. As stated above, we focus on the case where the cross section is shallow, $h_0 \ll w$. This induces two typical time scales for the exploration by the solutes of velocity variations perpendicular to the channel axis, exploration that they perform by thermal diffusion. These two time scales separate three regimes (see Figure 2): "very short" times, less than $O(h_0^2/D)$, during which solute only mildly samples the shorter transverse dimension,

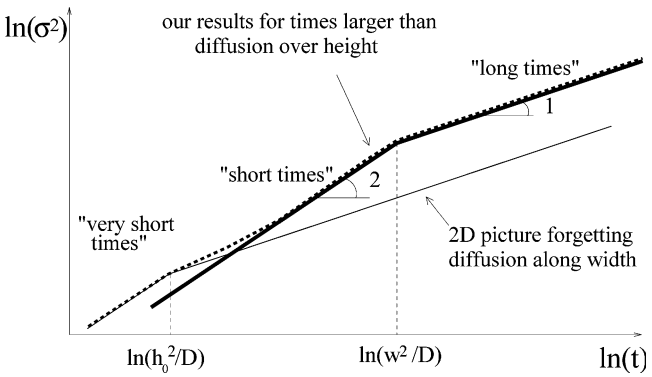

Figure 2. Schematic diagram of the increase of the variance in time. The thick solid curve corresponds to the short- and long-time regimes described in the text, where explicit formulas are given. The thin solid curve depicts dispersion arising from variations of the velocity along the height dimension, which is usually examined through a strictly two-dimensional study. The complete solution for the three-dimensional situation corresponds to the envelope (dashed) of the two curves and is thus well described by our approach for times longer than the crossover time between the two curves, which is $O(h_0^2/D)$.

"short" times, larger that $O(h_0^2/D)$ but less than $O(w^2/D)$, during which solute, having "equilibrated" in the short dimension starts to sample the longer transverse dimension, and eventually a "long" time regime, i.e., times longer than $O(w^2/D)$. If the thickness of the channel varies progressively along the largest transverse dimension, then the thickness-averaged velocities will vary noticeably from place to place (i.e., at different positions x along the width). These variations induce a hydrodynamic stretching extending throughout the short-time regime that adds up to the one corresponding to velocity heterogeneities in the thickness (Figure 2). Only in the long-time regime can molecular diffusion progressively reduce this "ballistic" hydrodynamic spreading by "averaging" throughout the cross section.

The reason the transverse variations of velocities along the width dominate the overall Taylor dispersivity is because the statistical averaging is poorer in that direction due to the longer diffusion time required. For a quasi-rectangular channel, there is little or no such transverse heterogeneity along the x direction of the height-averaged velocity (except for the vicinity of the side walls), so that this source of dispersion is weak or absent.

Main Results. To substantiate these qualitative statements, we now provide our analytical results, obtained, as detailed in the Appendix, by combining the method of moments applied to shallow channels as described in Aris[3] with a lubrication description of the flow field. Our results thus hold for smooth shallow cross-sectional shapes. The case of abrupt shape changes, as occurs for nearly rectangular shapes, is discussed in the section entitled Long-Time Dispersion for Quasi-Rectangular Shapes.

Long-Time Dispersivity. At long times, i.e., longer than $O(w^2/D)$, the spreading of the sample is effectively diffusive (Taylor−Aris dispersion). The average position is $\langle z\rangle = Vt$ and the variance, σ^2_{long}, grows linearly in time

$$\sigma^2_{\text{long}}(t) \simeq \langle (z - Vt)^2\rangle(t) \simeq 2D(1 + \kappa_1 Pe_w^2)t \qquad (5)$$

where Pe_w is the Péclet number defined using the width w as the relevant length scale (not h_0) and V as the mean velocity:

$$Pe_w = Vw/D \qquad (6)$$

This identification of the prominent role of the channel width is the first main point of our paper. The second is an explicit formula for the constant κ_1 in (5), which depends only on the nondimensional shape of the cross section as described by the function $H(X)$:

$$\kappa_1 = \frac{1}{4I_1}\int_{-1}^{1}\frac{1}{H(X)}\int_{-1}^{X}\left(H^2(X')\frac{I_1}{I_3} - 1\right)H(X')\,dX'\Big]^2 dX \qquad (7)$$

where we have introduced the short-hand notation

$$I_n = \int_{-1}^{1} H^n(X)\,dX \qquad (8)$$

This long-time behavior is fully described by the effective dispersion coefficient

$$D_{\text{eff}}^{\text{long}} = D(1 + \kappa_1 Pe_w^2) \qquad (9)$$

We emphasize that remarkably the channel height h_0 is completely absent in this long-time limit obtained for a smooth cross section (again abrupt shape changes, such as almost rectangular shapes are not included in this analysis).

Dispersion at Shorter Times. Due to its special relevance for microfluidic systems, we also investigate dispersion at shorter times, although the results are then not universal and depend on the initial distribution of solutes.

Of special interest is the "short" time regime, i.e., times scales longer than the (fast) time scale for molecular diffusion in the y direction but shorter than for that along the width of the channel; i.e., $O(h_0^2/D) < t < O(w^2/D)$. Then, differences along the width x of the height-averaged velocities lead to an effective diffusion coefficient increasing linearly in time. For initial distributions homogeneous along x, we explicitly obtain as described in the Appendix

$$D_{\text{eff}}^{\text{short}}(t) = \frac{1}{2}\frac{d}{dt}\sigma^2_{\text{short}}(t) \simeq D + \kappa_s V^2 t = D\left(1 + \kappa_s Pe_w^2 \frac{Dt}{w^2}\right) \qquad (10)$$

where κ_s is a dimensionless number that depends only on the nondimensional shape H of the cross section:

$$\kappa_s = I_1 I_5/I_3^2 - 1 \qquad (11)$$

Again, h_0 does not enter the description.

For even shorter times, i.e., shorter than $O(h_0^2/D)$, and for an initial distribution homogeneous in the cross section, a simple calculation using the lubrication description of the flow (eq 25 in the Appendix) yields a diffusivity formally similar to (10), with κ_s replaced by $\kappa_{vs} = (6I_1I_5/5I_3^2) - 1 = \kappa_s + (I_1I_5/5I_3^2)$.

Crossover Time. A useful outcome of the previous analysis is an estimate for the typical crossover time t_{xo} between hydrodynamic stretching and broadening by Taylor−Aris dispersion.

For large Péclet numbers ($Pe_w \gg 1$), equating the variance in the two regimes yieldsThis time scale, which as expected scales as

$$t_{xo} \simeq \frac{2\kappa_1}{\kappa_s}\frac{w^2}{D} = \kappa_{xo}\frac{w^2}{D} \tag{12}$$

the time to diffuse the width, sets the limit of validity of the long-time dispersive regime (eqs 6−10). Once again the channel width w is the important length scale.

In the above quantitative characterization of the dispersion process, three shape-dependent dimensionless numbers, κ_1, κ_s, and κ_{xo}, have been introduced. We calculate and tabulate these numbers for several representative shapes in the next section.

DISCUSSION

General Remarks. As is well known in the literature on hydrodynamic dispersion, the flow contributes a long-time effective diffusion that varies as the square of the average velocity. However, the channel dimension that enters the description is the width, not the height (assuming $h_0 \ll w$), a fact that is generally obscured since most analyses concern effectively two-dimensional situations. Furthermore, it is the square of that dimension that enters the expression of the long-time Taylor dispersion, so that we are actually arguing that, for channels of aspect ratio, w/h_0, of order 10, hydrodynamic dispersion is 100 times larger than an analysis based on the height would suggest! It is nevertheless worth noting that if the pressure drop Δp is specified for a channel of length L, then the mean velocity $V = (h_0^2 I_3 \Delta p/12 I_1 \mu L)$, where μ is the viscosity of the fluid; this feature brings the smallest dimension, the height, into the overall description.

The formulas above have been established using the lubrication approximation (see Appendix), so that we expect them to hold for arbitrary smooth and narrow cross sections. Note that although the examples quoted here mostly refer to the format common in microfluidics where one of the surface is flat (as described in Figure 1a), our results equally hold for any smooth narrow shape where the local height is $y_{max}(x) - y_{min}(x) = h(x)$. Also, the scaling forms are explicit in the formulas given above, so that we now turn to the computation of the numerical coefficients for a set of representative shapes.

Parabolic Cross-Sectional Shapes. Parabolic cross sections are commonly found in many microfluidic geometries based on soft lithography techniques (e.g., ref 8). Thus, we provide explicit results for such shapes by using the formulas of the previous section with $h(x) = h_0(1 - (x/w/2)^2)$ or $H(X) = 1 - X^2$. It is straightforward to evaluate the integrals in (7) to obtain

$$\kappa_1 = \frac{3347}{1081080} \approx 3.1 \times 10^{-3} \tag{13}$$

This value can immediately be compared with the more familiar $(1/4)(1/48) \approx 0.005$ for the well-known prefactor of the dispersivity for pressure-driven flows in a circular tube (the (1/4) factor stems from the comparison being made using the tube diameter, rather than the radius, in place of w). The short-time dispersivity is characterized by the constant $\kappa_s = (53/297) \approx 0.178$, so that the crossover coefficient (eq 12) from "ballistic" short-time to "diffusive" long-time dispersion is $\kappa_{xo} = (2\kappa_1/\kappa_s) = (3347/96460) \approx 0.035$.

One application of these ideas is to the quantitative description of the rotary mixer introduced by Quake and colleagues.[9] This device is commonly used to mix materials in one step of their processing in integrated systems using two-layer soft lithography. For such systems, the operation of active elements such as valves is favored by using smooth rounded cross sections, and fabrication often results in parabolic cross-sectional shapes of the channels. A typical microfluidic rotary mixer has a centerline radius $R = 1000\,\mu$m, width $w = 100\,\mu$m, height $h_0 = 10\,\mu$m, and mean velocity $V = 0.1$ cm/s. Therefore, if we take the molecular diffusivity to be $D \approx 5 \times 10^{-6}$ cm^2/s, then the crossover time for an experiment is typically $t_{xo} \approx 0.035w^2/D \approx 0.7$ s. This time scale should be compared with the average circulation time around the rotary mixer $2\pi R/V \approx 6$ s. Thus, well before a single revolution, the transport process is characterized by the description of dispersion based on the channel width. Our formulas can thus be used to refine the analysis presented by Squires and Quake,[10] where only one dimension was considered, and provides guidance for a complete 3D analysis of the problem along the lines of the 2D analysis presented by Gleeson et al.[11]

Other Simple Shapes. We have also computed the values of the nondimensional parameters κ_1, κ_s, and $\kappa_{xo} = 2\kappa_1/\kappa_s$ for elliptical and triangular cross sections, which are reported alongside those for the parabola in Table 1. The long-time result for the elliptical shape matches the limit of Aris's exact calculation (p 76 in ref 3).

Focusing on the long-time dispersivity, two facts are immediately apparent and worth emphasizing. First, as is common in such dispersion problems, the numbers are small for prefactors in a scaling theory, i.e., typically of order 10^{-3}−10^{-2}. Second, they are smaller (and so is dispersion) for flatter shapes, as is obvious following the sequence triangle → parabola → ellipse. This result corresponds to more uniform values of the velocity distribution, i.e., smaller gradients of the height-averaged velocities.

An extension of the above argument suggests making a connection to the case of the flattest shapes, i.e., rectangular shapes, for which exact (numerical) results are available. Blindly applying the above results with $h(x) = h_0$ leads to numerical values that are exactly zero for both the short- and long-time coefficients, as the height-averaged velocity is uniform. This result is at odds with existing calculations, but is logical in the framework of our approximations as we explain in the next subsection.

Long-Time Dispersion for Quasi-Rectangular Shapes. To establish the connection between our analysis for smooth shapes and the rectangle (which is not smooth as $h(x)$ goes abruptly from h_0 to 0 on the two sides), we consider dispersion in quasi-rectangular channels (Figure 3, top), which are flat for $|x| < w/2 - \lambda$ and then monotonically tend to zero over the length λ. In addition to providing a connection to the case of a rectangle, the topic is of interest on its own, as this kind of channel shape is indeed found in some microfluidic systems.[7] We start by general

(8) Unger, M. A.; Chou, H. P.; Thorsen, T.; Scherer, A.; Quake, S. R. *Science* **2000**, *288*, 113−116.

(9) Chou, H. P.; Unger, M. A.; Quake, S. R. *Biomed. Microdevices* **2001**, *3*, 323−330.

(10) Squires, T. M.; Quake, S. R. *Rev. Mod. Phys.* In press.

(11) Gleeson J. P.; Roche O. M.; West J.; Gelb A. *SIAM J. Appl. Math.* **2004**, *64*, 1294−1310.

Table 1. Coefficients κ_1, κ_s, and κ_{xo} According to the Lubrication Approach for Shallow Cross-Sectional Shapes (Height h_0 and Width w with $h_0 \ll w$)

cross-sectional shape	κ_1	κ_s	$\kappa_{xo} = 2\kappa_1/\kappa_s$	D_{eff}^{long}
triangle	$1/192 \approx 0.0052$	$1/3 \approx 0.333$	$1/32 = 0.031$	$D + 0.0052(V^2w^2/D)$
parabola	$3347/1081080 \approx 0.0031$	$53/297 = 0.178$	$3347/96460 \approx 0.035$	$D + 0.0031(V^2w^2/D)$
ellipse	$5/2304 \approx 0.0022$	$1/9 \approx 0.111$	$5/128 \approx 0.039$	$D + 0.0022(V^2w^2/D)$

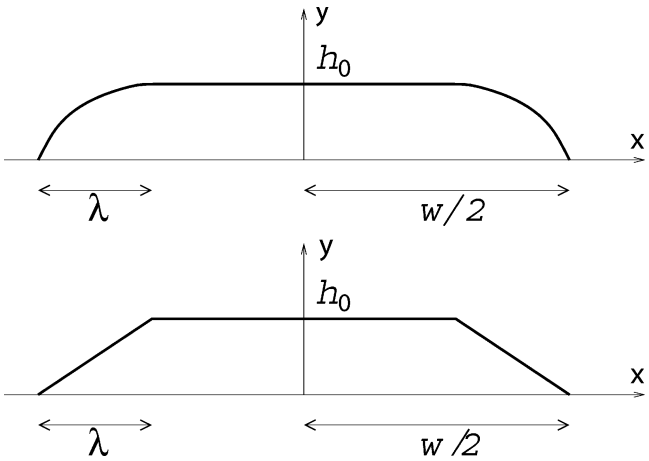

Figure 3. Quasi-rectangular cross-sectional shapes.

considerations that hold irrespective of the shape of the two (smooth) "wings", before providing an explicit illustration for the case of triangular end pieces (Figure 3, bottom). To be specific, in the discussion below we assume $h_0 \le \lambda \le w/2$.

Recall that dispersion is controlled by transverse diffusion, which samples the velocity distribution. For the general quasi-rectangular cross-sectional shape, the depth-averaged velocity is the same throughout the central flat region and variations are restricted to a region of size λ near the side walls, which then controls the dispersion. Indeed, the nondimensional coefficient κ_1, now dependent on λ/w, can be shown from eq 7 to behave as

$$\kappa_1\left(\frac{\lambda}{w}\right) = \frac{\lambda^2}{w^2} f\left(\frac{\lambda}{w}\right) \tag{14}$$

where $f(\lambda/w)$ is an $O(1)$ function with finite limits for $\lambda/w \to 0$ and $\lambda \to w/2$. Thus, when $\lambda = O(w)$, as outlined above the dispersive correction $O(\kappa_1 Pe_w^2)$ is controlled by the width of the channel. In contrast, in the limit $\lambda \ll w$ or $\lambda/w \to 0$, the depth-averaged velocity only varies on a scale λ near the boundaries and $\kappa_1 \approx (\lambda/w)^2 f(0)$. This implies that the dispersion, proportional to $\kappa_1 Pe_w^2 = f(0)(V\lambda/D)^2$, is independent of the width of the channel and is controlled by the small region of size λ in the neighborhood of the corner!

At the limit of validity of our formalism, we take $\lambda = O(h_0 \ll w)$ and observe that for nearly rectangular channels the dispersive contribution becomes $O(Pe_h^2)$, where $Pe_h = Vh_0/D$; the dispersion now depends completely on the channel height (not the width). This result is known in the literature on dispersion in rectangular channels $D_{eff}^{long}/D \approx 8(1/210)Pe_h^2$ (e.g., refs 12 and 13), with in that case the side walls yielding only a prefactor change (not a scaling one) to the 2D result $D_{eff}^{long}/D \approx (1/210)Pe_h^2$. However, as we have demonstrated in this paper, this is not true for generic shallow microchannels.

To illustrate these points, we consider a special class of shapes that are rectangular in the middle and triangular near the end (see Figure 3). As the triangular region of width λ is diminished, the cross section approaches a rectangle of height h_0 and width w. So, we utilize the dimensionless shape function involving the parameter ϵ, $0 \le \epsilon = \lambda/(w/2) \le 1$,

$$H(X) = \begin{cases} 1 & \text{for } 0 \le |X| \le 1-\epsilon \\ \dfrac{1-|X|}{\epsilon} & \text{for } 1-\epsilon \le |X| \le 1 \end{cases} \tag{15}$$

Each of the necessary integrals in eqs 7 and 8 for the dispersion can now be evaluated; e.g., $I_1 = 2(1 - {}^1/_2\,\epsilon)$, $I_3 = 2(1 - {}^3/_4\,\epsilon)$, $I_5 = 2(1 - {}^5/_6\,\epsilon)$, etc. After some algebra we find that $\kappa_1(\epsilon)$ has the form

$$\kappa_1(\epsilon) = \frac{\epsilon^2}{192}\,\frac{(32 - 52\epsilon + 20\epsilon^2 + \epsilon^3)}{(2-\epsilon)(4-3\epsilon)^2} \tag{16}$$

in the limit $\epsilon \to 1$, the cross section is a triangle, and we indeed recover $\kappa_1(\epsilon \to 1) = 1/192$ as given in Table 1. In contrast, in the limit $\lambda \ll w$ or $\epsilon \to 0$, $\kappa_1 \approx \epsilon^2/192$, or a dispersion for high Péclet numbers that is $\kappa_1 Pe_w^2 = 1/48\ (V\lambda/D)^2$. Extrapolating this result to $\lambda \sim h_0$ provides a result consistent with the magnitude and scaling of the dispersivity for rectangular cross sections. However, here we reach the limits of our approximations, so that to produce exact results for such shapes, the detailed velocity distribution in the corner needs to be known (e.g., refs 12 and 13), and a full three-dimensional analysis is necessary.

ACKNOWLEDGMENT

H.A.S. thanks the Harvard MRSEC for support and the City of Paris and the Laboratoire de Physico-Chimie Théorique of ESPCI for support during a sabbatical visit. We thank the Institut d'Etudes Scientifiques de Cargese for providing a pleasant and stimulating environment in which this work was initiated.

APPENDIX: MATHEMATICAL DERIVATIONS OF THE MAIN RESULTS BY ARIS'S METHOD OF MOMENTS

In this Appendix, we first outline a procedure already followed by Aris at the end of his seminal paper,[3] which led him to a general formula for the long-time dispersion in shallow channels. We then describe the additional steps we take to obtain the results presented in the text, i.e., making use of the lubrication ap-

(12) Doshi, M. R.; Dalya, P. M.; Gill, W. N. *Chem. Eng. Sci.* **1978**, *33*, 795−804.
(13) Chatwin, P. C.; Sullivan, P. J. *J. Fluid Mech.* **1982**, *120*, 347−358.

proximation and solving for the short-time behavior for a special class of initial conditions.

Starting from the convection−diffusion eq 2, the first step in the analysis of the transport problem is to use the approximation $h_0 \ll w$ to derive a simplified equation for quantities averaged along the short transverse direction y. It is convenient to define the transverse averages

$$\bar{u}(x) = \frac{1}{h(x)} \int_0^{h(x)} u(x, y)\, dy \tag{17}$$

$$\bar{c}(x, z, t) = \frac{1}{h(x)} \int_0^{h(x)} c(x, y, z, t)\, dy \tag{18}$$

Here we have assumed, as sketched in Figure 1, the most common situation in microfluidics, which is that the channel is closed on one side by a flat plate so that the channel boundaries are at $y = 0$ and $y = h(x)$. Any other smooth shape described by $y_{min}(x)$ and $y_{max}(x)$ with $y_{max}(x) - y_{min}(x) = h(x)$ leads to identical results in the present frame of approximations.

The evolution equation for $\bar{c}(x, z, t)$, which is adequate to describe evolution at time scales longer than h_0^2/D, is

$$\frac{\partial \bar{c}}{\partial t} + \bar{u} \frac{\partial \bar{c}}{\partial z} = D \frac{\partial^2 \bar{c}}{\partial z^2} + \frac{D}{h(x)} \frac{\partial}{\partial x} \left(h(x) \frac{\partial \bar{c}}{\partial x} \right) \tag{19}$$

with the boundary conditions $\partial \bar{c}/\partial x\ (x = \pm w/2, z, t) = 0$, and an arbitrary initial condition $\bar{c}(x, z, t = 0)$, which is normalized for simplicity so that $\int dx\, h(x) \int dz \bar{c}(x, z, t = 0) = 1$ (which then obviously holds for any time).

We can now follow the methods of moments developed by Aris[3] and inspect the evolution of the quantities (or moments), defined as

$$c_n(x, t) = \int \bar{c}(x, z, t) (z - Vt)^n\, dz \tag{20}$$

In particular, the first two moments evolve according to

$$\frac{\partial c_0}{\partial t} = D \frac{1}{h(x)} \frac{\partial}{\partial x} \left(h \frac{\partial c_0}{\partial x} \right) \tag{21}$$

$$\frac{\partial c_1}{\partial t} = (\bar{u}(x) - V) c_0(x, t) + D \frac{1}{h(x)} \frac{\partial}{\partial x} \left(h \frac{\partial c_1}{\partial x} \right) \tag{22}$$

with $(\partial c_n/\partial x)\ (x = \pm w/2, t) = 0$. The variance $\sigma^2(t) = \langle (z - Vt)^2 \rangle (t) = \int dx h(x) c_2(x, t)$ evolves as

$$\frac{d}{dt} \langle (z - Vt)^2 \rangle = 2D + 2 \int dx h(x) (\bar{u}(x) - V) c_1(x, t) \tag{23}$$

Whatever the initial conditions, as time goes on, $c_0(x, t)$ tends toward a constant value $c_0(t \to \infty) = c_0^\infty = (\int dx\ h(x))^{-1}$, and consequently, $c_1(x, t)$ tends toward a steady profile $c_1(x, t \to \infty) = c_1^\infty(x)$ given by This result can be used in (23) to compute the

$$D \frac{d}{dx} \left(h(x) \frac{dc_1^\infty}{dx} \right) = - c_0^\infty h(x)\ (\bar{u}(x) - V) \tag{24}$$

long-time dispersivity through a shape-dependent integral, as already recognized by Aris (with slightly different notations), and used by him for the case of ellipses. We now take a few additional steps.

(i) The main step is to use the lubrication approximation to relate the flow pattern $\bar{u}(x)$ to the shape. Within the lubrication approximation $u(x, y) = Ay(h(x) - y)$ with A a constant proportional to the pressure gradient, so that we find

$$\bar{u}(x) = \frac{I_1 h^2(x)}{I_3 h_0^2} V \tag{25}$$

where the constants I_n are defined in eq 8.

(ii) Long-time regime: Then we introduce the intermediate function

$$g(x) = \int_{-w/2}^{x} dx' h(x') (\bar{u}(x') - V) \tag{26}$$

to obtain from eqs 23 and 24, through an integration by parts (note that $g(\pm w/2) = 0$),

$$\frac{d}{dt} \langle (z - Vt)^2 \rangle = 2D \left(1 + \frac{\int dx [g^2(x)/h(x)]}{\int dx h(x)} \right) \tag{27}$$

Inserting in this equation the lubrication flow field (25) and extracting from the integrals the dimensional quantities using $h = h_0 H(2x/w)$ yields the final results given as eq 7 in the main body of the paper for the long-time regime.

(iii) Short-time regime: In addition, to get partial insight into the "short-time" regime where homogenization along y is effective but not that along x, we focus on a solvable family of cases, namely that of initial conditions independent of x: $\bar{c}(x, z, t = 0) = f(z)$. In that limit, given the normalization chosen $c_0(x, t)$ is a constant in space and time $c_0(x, t) = (\int dx h(x))^{-1}$, and $c_1(x, t = 0) = 0$ if the origin of the z axis is chosen at the initial location of the center of mass of the distribution $\int dz f(z) = 0$. Then for times shorter than the diffusion time across the channel $t < O(w^2/D)$, it is clear that we have the simple approximation $c_1(x, t) \simeq (\int dx\, h(x))^{-1} (\bar{u}(x) - V)t$. Thus, the evolution of the variance follows from eq 23:

$$\frac{d}{dt} \langle (z - Vt)^2 \rangle = 2D + 2 \frac{\int dx\, h(x) (\bar{u}(x) - V)^2}{\int dx\, h(x)} t \tag{28}$$

Inserting the flow field in the lubrication approximation 25 yields the "short-time" result quoted in the text.

Received for review May 18, 2005. Accepted October 18, 2005.

AC0508651